

Nonstoichiometric Interfaces and Al_2O_3 Adhesion with Al and Ag

W. Zhang¹ and J. R. Smith²

¹*Princeton Materials Institute, Princeton University, Princeton, New Jersey 08540*

²*Delphi Research Laboratories, Warren, Michigan 48090*

(Received 2 May 2000)

We have determined the relative stability of stoichiometric, oxygen-rich, and aluminum-rich Al/ Al_2O_3 and Ag/ Al_2O_3 interfaces from first principles. Stable structures vary significantly with oxygen chemical potentials. Computed works of adhesion agree reasonably well with sessile drop experimental values, including correlation with measured oxygen chemisorption effects on Ag. The ordering of predicted bond energies of the interfaces, ceramics, and metals seems consistent with monotonic and fatigue fracture experiments.

PACS numbers: 68.35.-P, 82.65.Dp

Metal/alumina interfaces have been the subject of considerable research of late (see, e.g., [1–14]). This is due in part to the importance of these interfaces in structural composites, electronic packaging, and corrosion-resistant coatings.

Recently it has been observed [1–3] that metal/alumina interfaces can deviate from stoichiometry (at stoichiometry, the ratio of numbers of oxygen to aluminum atoms is 3 to 2), depending on the oxygen partial pressure. Moreover, the data suggest that the work of adhesion W_{Ad} varies significantly with deviations from stoichiometry.

We consider here interfaces of alumina with Al and Ag for two reasons. First, they are commonly found in the aforementioned applications. Second, they are on nearly opposite ends of the range of oxide heats of formation [15]. In the following, we provide the first computational results for these interfaces which allow deviations from stoichiometry. This includes for the first time the variation of W_{Ad} with interfacial oxygen or aluminum enrichment for these interfaces (and, to our knowledge, for any metal/alumina interface).

Our first principles, fully self-consistent electronic structure computations were performed with an accurate, full potential linearized augmented plane wave method [16,17]. The atomic structures were fully relaxed in all dimensions by minimizing the Hellmann-Feynman force [18] on every atom. The generalized-gradient approximation of Perdew *et al.* [19] was employed for exchange-correlation interactions. Other technical details of our computational methods are described fully in Ref. [20(a)].

Transmission electron microscopy (TEM) data on the Cu/ Al_2O_3 interface [21] shows a preferred Cu(111) on the Al_2O_3 (0001) orientational relationship. While we are not aware of any such TEM data for the Al/ Al_2O_3 and Ag/ Al_2O_3 interfaces, because these are all fcc metals we will assume the same orientational relationship. For the [0001] direction of Al_2O_3 , each layer of oxygen atoms is sandwiched between single layers of aluminum atoms. The atom density in the oxygen layers is 3 times that in the aluminum layers, preserving stoichiometry. The stoichiometric alumina surface or interface is denoted as $(\text{Al}_2\text{O}_3)_{\text{Al}}$,

since a single plane of Al atoms terminates it. We will also consider an oxygen-rich alumina surface or interface designated as $(\text{Al}_2\text{O}_3)_{\text{O}}$, terminated by a single oxygen layer. An aluminum-rich surface or interface that we will consider is denoted as $(\text{Al}_2\text{O}_3)_{\text{Al}_2}$, terminated by two planes of Al atoms. It is now known [11] that for the clean Al_2O_3 (0001) surface the stoichiometric surface $(\text{Al}_2\text{O}_3)_{\text{Al}}$ is stable over a broad range of oxygen chemical potentials or partial pressures. Here we identify the stable configurations at the metal/alumina interfaces.

We determine the interfacial energy, because the stable interfacial structure minimizes the interfacial energy. If we are to allow the interfaces to be oxygen rich or oxygen poor, then we must take into account the effects of variations in oxygen availability and, correspondingly, variations in oxygen chemical potential. We do this via the methodology of Ref. [20(a)] (see, in particular, Sec. III C).

Results for the interface energy are plotted in Fig. 1(a) for Ag/ Al_2O_3 and Fig. 1(b) for Al/ Al_2O_3 . For each alumina termination, we considered three starting configurations for the Ag or Al atoms relative to the alumina surface, reached by (effectively) sliding the Ag or Al slab along the alumina surface. These are for the Ag or Al atoms residing atop O atoms, atop the three Al sites in the Al_2O_3 structure, or atop the threefold O “hollow” sites. For each starting configuration, the metal or alumina atoms were allowed to fully relax as discussed above. In this way, the overall lowest-energy interfacial structure was found.

Let us first look at the results for the stoichiometric interfaces Ag/ $(\text{Al}_2\text{O}_3)_{\text{Al}}$ and Al/ $(\text{Al}_2\text{O}_3)_{\text{Al}}$. The results are independent of oxygen chemical potential μ_{O} , as expected. We see that the lowest energy configuration for Ag/ $(\text{Al}_2\text{O}_3)_{\text{Al}}$ is for the Ag atoms atop the hollow sites, while that for Al/ $(\text{Al}_2\text{O}_3)_{\text{Al}}$ is for the Al metal atoms atop the Al sites. But the interfacial energies do not vary substantially between the three configurations.

For both Al-rich terminations Ag/ $(\text{Al}_2\text{O}_3)_{\text{Al}_2}$ and Al/ $(\text{Al}_2\text{O}_3)_{\text{Al}_2}$, the interfacial energies are higher than that for the respective stoichiometric interface, indicating the latter is more stable. For both oxygen-terminated interfaces Ag/ $(\text{Al}_2\text{O}_3)_{\text{O}}$ and Al/ $(\text{Al}_2\text{O}_3)_{\text{O}}$, the atop-Al-site

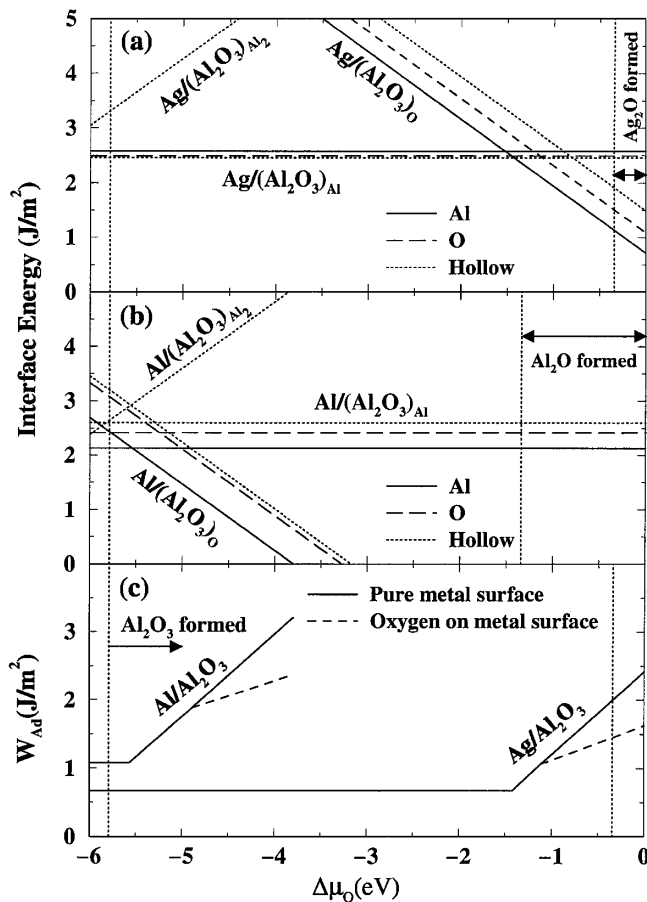


FIG. 1. Interfacial energies and works of adhesion W_{Ad} versus $\Delta\mu_O \equiv \mu_O - \mu_O^{\text{gas}}$, i.e., versus the difference between the oxygen chemical potential in the material and its value [20(a)] for the ambient gas μ_O^{gas} . Interfaces are defined in the text. The three metal site locations are indicated by solid, dashed, and dotted curves. Vertical dotted lines are located at oxygen chemical potential values for which bulk oxides could form as indicated.

configuration is the most stable. In this case, there is substantial rumpling of the metal layer closest to the oxygen layer, such that one of every three of the metal atoms occupies the site of the missing Al of the (Al₂O₃)_O. Both oxygen-terminated interfaces become more stable than the respective stoichiometric interface for sufficiently large oxygen chemical potentials. This is particularly interesting because, as noted above, for the free Al₂O₃(0001) surface the stoichiometric surface is stable. Thus adhesion can reverse the stable structure.

Note the vertical dotted lines in Fig. 1. They indicate the values of $\Delta\mu_O \equiv \mu_O - \mu_O^{\text{gas}}$ at which the specified bulk oxides can begin to form. For $\Delta\mu_O < -5.79$ eV, Al₂O₃ tends to become Al, so that range would not be of interest. From Fig. 1 one can conclude that if Al/Al₂O₃ interfaces are formed, they will very likely be oxygen rich, i.e., Al/(Al₂O₃)_O. It is well known [7,8] that Al/Al₂O₃ interfaces can, in fact, be formed.

The interfacial energy of the Ag/(Al₂O₃)_O interface falls below that of the (stoichiometric) Ag/(Al₂O₃)_{Al} interface at a substantially higher value of $\Delta\mu_O$. This is to be expected, since the oxide heat of formation of Ag₂O is known [15] to be substantially smaller than that of Al₂O₃. The results shown in Fig. 1 suggest that one might expect to find either Ag/(Al₂O₃)_{Al} or Ag/(Al₂O₃)_O, depending on the oxygen chemical potential or partial pressure.

Now that we know the interfacial energy γ_I as a function of the oxygen chemical potential, as shown in Figs. 1(a) and 1(b), we can determine the work of adhesion W_{Ad} as

$$W_{Ad} = \sigma_M + \sigma_{\text{Al}_2\text{O}_3} - \gamma_I, \quad (1)$$

where σ_M is the surface energy of the metal surface and $\sigma_{\text{Al}_2\text{O}_3}$ is the alumina surface energy. W_{Ad} is the metal/alumina bond energy per cross sectional area. Our results for the Al(111), Ag(111), and Al₂O₃(0001) surface energies are shown near the bottom of Table I. One can see there is reasonable agreement between the predicted and the measured surface energies. Results for W_{Ad} are plotted in Fig. 1(c). They are determined from Eq. (1) and the lowest γ_I value at each $\Delta\mu_O$. The lowest γ_I value is chosen because W_{Ad} is defined for the stable interface. Note that when that stable interface is stoichiometric, i.e., Al/(Al₂O₃)_{Al} and Ag/(Al₂O₃)_{Al}, W_{Ad} is independent of $\Delta\mu_O$ as expected. However, when the interface becomes oxygen terminated, i.e., Al/(Al₂O₃)_O and Ag/(Al₂O₃)_O, W_{Ad} rises with $\Delta\mu_O$.

Next we attempt to estimate the effect of oxygen chemisorption on W_{Ad} . If a chemisorbed layer of oxygen appears on the metal surfaces, it will lower σ_M and, by Eq. (1), W_{Ad} . Oxygen will appear on the surface of the metal if segregation of oxygen to the surface is exothermic. Let us define E_d as the desorption energy of the chemisorbed oxygen. Then by the preceding arguments, oxygen will segregate to the surface if $\Delta\mu_O > -E_d$. We carried out chemisorption computations of E_d for oxygen on Al(111) and Ag(111), using the same methods described above that we applied to the metal/alumina interfaces. Consistent with experiment [24,25], adsorbed oxygen atoms were distributed over the fcc sites. Our results for desorption energies E_d and equilibrium oxygen/metal distances d are given in Table II. Also shown there are theoretical and experimental results of others for comparison. Reasonable agreement is obtained. If N_s is the number of surface sites in a monolayer and Θ_O is the fraction of them filled with chemisorbed oxygen atoms, then [28] $\Delta\sigma_M = -N_s\Theta_O(\Delta\mu_O + E_d) = \Delta W_{Ad}$. The dashed lines in Fig. 1(c) result from computing $\Delta\sigma_M = \Delta W_{Ad}$ with an assumed $\Theta_O = \frac{1}{3}$.

Next let us compare these predictions with experimental observations. Sessile drop experiments [1–4] to measure W_{Ad} are done at low oxygen partial pressures since there must be no oxide film on the molten metal drop affecting the measured contact angle. One can see from Fig. 1(c) that for a successful sessile drop experiment on

TABLE I. Works of separation in J/m^2 . Interfaces are as defined in the text. Surface energies for Al(111), Ag(111), and $Al_2O_3(0001)$ can be obtained from the corresponding last three values in the table by dividing by 2. The $Al_2O_3(0001)$ is Al-terminated, appropriate to the ground state [11].

Interface	Theory	Experiment
Al/ $(Al_2O_3)_{Al}$	1.078	1.070 ^a , 0.955 ^b
Ag/ $(Al_2O_3)_{Al}$	0.672	0.500 ^c
Al/ $(Al_2O_3)_O$	10.095	
Ag/ $(Al_2O_3)_O$	4.649	
Al/ $(Al_2O_3)_{Al_2}$	1.433	
Ag/ $(Al_2O_3)_{Al_2}$	0.679	
Al/Al	2.118	2.340 ^d
Ag/Ag	1.958	1.820 ^e , 3.080 ^d
Al_2O_3/Al_2O_3	4.300	4.6 ^e

^aReference [3]; ^bRef. [2]; ^cRef. [4]; ^dRef. [22]; ^eRef. [23].

Al/ Al_2O_3 , $\Delta\mu_O$ must be [1] approximately -5.79 eV, where the clean metal drop surface and the alumina surface can coexist. Thus for Al/ Al_2O_3 , the correct interface whose computed W_{Ad} is to be compared with sessile drop experiments is Al/ $(Al_2O_3)_{Al}$. This is given by the horizontal part of the curve in Fig. 1(c) and in Table I. One can see from a comparison with the experimental values listed in Table I that the agreement is reasonably good. As noted above, for Ag/ Al_2O_3 one might expect to find either the stoichiometric or the oxygen-rich interface, depending on oxygen partial pressure or $\Delta\mu_O$. This is because both interfaces are predicted to arise below the $\Delta\mu_O$ value at which Ag_2O is formed. In fact, the W_{Ad} curve for Ag/ Al_2O_3 shown in Fig. 1(c) is similar to the sessile drop experimental W_{Ad} results plotted in Fig. 5 of Ref. [4]. This suggests that the relatively high oxygen activities (oxygen activity [4] is the oxygen partial pressure in atmospheres), at which the Ag/ $(Al_2O_3)_O$ interface becomes stable can be reached in a sessile drop experiment for this system. Note, moreover, that the measurements of Ref. [4] indicate that effects of oxygen on the Ag surface contribute to a lowering of W_{Ad} , but despite that there is a net increase of W_{Ad} with increasing oxygen activity. These experimental observations are all consistent with our predictions shown in Fig. 1(c).

For the low $\Delta\mu_O$ regime at which Ag/ $(Al_2O_3)_{Al}$ is stable, the experimental data [4] show an interesting step,

TABLE II. Oxygen desorption energies E_d (eV) and vertical distance d (angstroms) between chemisorbed oxygen and surface plane of the metal atoms.

Substrate	E_d	d
Al(111)	4.9 ^a , 5.0 ^b	0.75 ^a , 0.6–0.7 ^c , 0.87 ^b
Ag(111)	1.1 ^a , 0.8 ^d	1.2 ^a , 1.4 ^d

^aComputed here; ^bRef. [26]; ^cRef. [25] (experiment); ^dRef. [27].

which the authors acknowledge requires further experimentation to obtain a better understanding of this feature. Our W_{Ad} value for Ag/ $(Al_2O_3)_{Al}$, which is shown as the horizontal part of the plot in Fig. 1(c) and in Table I, roughly agrees with the larger of the two values in the experimental stepped region, Fig. 5 of Ref. [4], as can be seen in Table I. Comparison of Figs. 1 and 4 of Ref. [4] show that for Ag/ Al_2O_3 the measurements indicate that the Ag surface energy begins to decrease due to oxygen chemisorption at an oxygen activity near that at which the measured W_{Ad} begins to increase. This is consistent with our predictions in Fig. 1(c).

Results for works of separation can be found in Table I. The work of separation is defined as the energy of the interfacial bonds where in the final, separated state the surfaces have the same termination as they had in the initial, bonded state. For example, for Al/ $(Al_2O_3)_O$ the final state alumina surface termination is $(Al_2O_3)_O$. For Al/ $(Al_2O_3)_{Al}$ the final state is $(Al_2O_3)_{Al}$, which is the stable surface structure, so in that case the work of separation is equal to W_{Ad} . One would expect works of separation to apply to rapid processes such as ordinary fracture processes, while W_{Ad} would apply to stable processes such as sessile drop experiments. This is because stable processes would allow time for the free surfaces to revert to their stable structures. While fracture is a complex process involving more than bond breaking, one might hope nevertheless to gain some insight from bond energies. Finally, note that the works of separation for the oxygen-terminated interfaces are substantially larger than those for the stoichiometric interfaces.

We noted above that Al/ Al_2O_3 interfaces are likely to be oxygen rich, i.e., Al/ $(Al_2O_3)_O$. Thus for sufficiently rapid processes such as perhaps fracture, one would expect increasing interfacial bond energies to be in the order (Table I) Al/Al < Al_2O_3/Al_2O_3 < Al/ Al_2O_3 . This appears to be consistent with experimental observations (see Dalgleish *et al.* [7] and references therein), that (monotonic) fracture of Al/ Al_2O_3 interfaces never occurs via interface cracking, but rather the junction fails either in the Al or the Al_2O_3 . McNaney *et al.* [8] found from their fatigue-crack growth studies that for relatively high driving forces (and hence higher crack velocities), the Al/ Al_2O_3 junction tended to fail in the Al, consistent with the monotonic fracture studies [7] and our predicted ordering given above for that process. However, they found for lower driving forces their fatigue failures were occurring at the Al/ Al_2O_3 interface. Perhaps for the lower driving forces the cracks are moving slowly enough so that the ordering is determined by W_{Ad} . In this case one can see from Fig. 1(c) and Table I that the ordering can be Al/ Al_2O_3 < Al/Al < Al_2O_3/Al_2O_3 . This appears consistent with the experimental findings of McNaney *et al.* [8].

Finally, fracture experiments have indicated (see Gaudette *et al.* [8] and references therein), that Al/ Al_2O_3 interfaces are particularly strong relative to many other

metal/ Al_2O_3 interfaces, including $\text{Ag}/\text{Al}_2\text{O}_3$. This is consistent with the $\text{Ag}/(\text{Al}_2\text{O}_3)_\text{O}$ work of separation being less than half of that of $\text{Al}/(\text{Al}_2\text{O}_3)_\text{O}$, as listed in Table I.

In conclusion, these first computations show that the stable structures of $\text{Al}/\text{Al}_2\text{O}_3$ and $\text{Ag}/\text{Al}_2\text{O}_3$ interfaces vary significantly with the oxygen chemical potential. While the free $\text{Al}_2\text{O}_3(0001)$ surface is Al terminated, the $\text{Al}/\text{Al}_2\text{O}_3$ interface is oxygen terminated except at the lowest oxygen potentials and the $\text{Ag}/\text{Al}_2\text{O}_3$ interface is Al terminated up to the relatively high oxygen potentials at which it switches to oxygen terminated. These results appear to be consistent with the substantially larger heats of oxide formation for Al compared to Ag. Computed W_{Ad} values agree reasonably well with sessile drop experimental values. In fact, the near coincidence of the onset of oxygen chemisorption on Ag and the onset of the rise of W_{Ad} with chemical potential seen in our computations is mirrored in the experimental data. Finally, the ordering of predicted bond energies for the metals, ceramics, and metal/ceramic interfaces appears consistent with the results of monotonic fracture, fatigue fracture, and sessile drop experiments.

The authors acknowledge, with thanks, numerous useful conversations with Professor Anthony Evans, including the formulation of plans for computations and the relation of our results to experimental results. We also thank Dr. Roland Cannon for his guidance on oxygen partial pressures and stoichiometry. This work was supported in part by the NSF, under Grant No. NSF DMR9-98-05188.

-
- [1] E. Saiz, R. M. Cannon, and A. O. Tomsia, *Acta Mater.* **47**, 4209 (1999).
- [2] D. Chatain, L. Coudurier, and N. Eustathopoulos, *Rev. Phys. Appl.* **23**, 1055 (1988).
- [3] V. Merlin and N. Eustathopoulos, *J. Mater. Sci.* **30**, 3619 (1995).
- [4] D. Chatain, F. Chabert, V. Ghetta, and J. Fouletier, *J. Am. Ceram. Soc.* **77**, 197 (1994).
- [5] J. Bruley, R. Brydson, H. Mulleejans, J. Mayer, G. Gutekunst, W. Mader, D. Knauss, and M. Ruhle, *J. Mater. Res.* **9**, 2574 (1994).
- [6] P. Blochl, G. P. Das, H. F. Fischmeister, and U. Schonberger, in *Metal-Ceramic Interfaces*, edited by M. Ruhle, A. G. Evans, M. F. Ashby, and J. P. Hirth (Pergamon Press, Oxford, 1990), p. 9.
- [7] A. G. Evans and B. J. Dalgleish, *Acta Metall. Mater. Suppl.* **40**, S295 (1992); see also B. J. Dalgleish, K. P. Trumble, and A. G. Evans, *Acta Metall.* **37**, 1923 (1989); A. G. Evans, J. W. Hutchinson, and Y. Wei, *Acta Mater.* **47**, 4093 (1999).
- [8] F. G. Gaudette, S. Suresh, and A. G. Evans, *Metall. Mater. Trans. A, Phys. Metall. Mater. Sci.* **30**, 763 (1999); see also J. M. McNaney, R. M. Cannon, and R. O. Ritchie, *Acta Mater.* **44**, 4713 (1996).
- [9] T. Hong, J. R. Smith, and D. J. Srolovitz, *Acta Metall. Mater.* **43**, 2721 (1995).
- [10] I. Manassidis and M. J. Gillan, *J. Am. Ceram. Soc.* **2**, 335 (1994); see also J. Guo, D. E. Ellis, and D. J. Lam, *Phys. Rev. B* **45**, 13 647 (1992); *J. Am. Ceram. Soc.* **77**, 398 (1994).
- [11] R. Di Felice and J. E. Northrup, *Phys. Rev. B* **60**, R16287 (1999); see also X.-G. Wang, A. Chaka, and M. Scheffler, *Phys. Rev. Lett.* **84**, 3650 (2000).
- [12] C. Kruse, M. W. Finnis, V. Y. Milman, M. C. Payne, A. De Vita, and M. J. Gillan, *J. Am. Ceram. Soc.* **77**, 431 (1994); see also I. G. Batirev, A. Alavi, M. W. Finnis, and T. Deutsch, *Phys. Rev. Lett.* **82**, 1510 (1999).
- [13] G. L. Zhao, J. R. Smith, J. Reynolds, and D. J. Srolovitz, *Interface Sci.* **3**, 289 (1996).
- [14] C. Verdozzi, D. J. Jennison, P. A. Schultz, and M. P. Sears, *Phys. Rev. Lett.* **82**, 799 (1999); see also A. Bogicevic and D. R. Jennison, *Phys. Rev. Lett.* **82**, 4050 (1999); C. Elsaesser (to be published).
- [15] *CRC Handbook of Chemistry and Physics*, edited by D. R. Lide (CRC Press, Boca Raton, FL, 1997), 78th ed., pp. 5–6.
- [16] E. Wimmer, H. Krakauer, M. Weinert, and A. J. Freeman, *Phys. Rev. B* **24**, 864 (1981).
- [17] P. Blaha, K. Schwarz, P. Sorantin, and S. B. Trickey, *Comput. Phys. Commun.* **59**, 399 (1990); P. Blaha, K. Schwarz, and J. Luitz, WIEN97 (Vienna University of Technology, Vienna, 1997); D. Singh, *Plane Waves, Pseudopotentials and the LAPW Method* (Kluwer Academic Publishers, Dordrecht, The Netherlands, 1994).
- [18] W. Kohler, S. Wilke, M. Scheffler, R. Kouba, and C. Ambrosch-Draxl, *Comput. Phys. Commun.* **94**, 31 (1996).
- [19] J. P. Perdew, K. Burke, and M. Ernzerhof, *Phys. Rev. Lett.* **77**, 3865 (1996).
- [20] (a) W. Zhang and J. R. Smith, *Phys. Rev. B* **61**, 16 883 (2000); (b) see also W. Zhang and J. R. Smith, *Phys. Rev. Lett.* **82**, 3105 (1999).
- [21] G. Dehm, M. Ruhle, G. Ding, and R. Raj, *Philos. Mag. B* **71**, 1111 (1995).
- [22] H. Wawra, *Z. Metallkd.* **66**, 395 (1975); **66**, 492 (1975).
- [23] D. A. Weirauch, Jr. and P. Darrell Ownby, *J. Adhes. Sci. Technol.* **13**, 1321 (1999).
- [24] V. Zhukov, I. Popova, and J. T. Yates, Jr., *Surf. Sci.* **441**, 251 (1999).
- [25] F. Bautier de Mongeot, U. Valbusa, and M. Rocca, *Surf. Sci.* **339**, 291 (1995).
- [26] J. Jacobsen, B. Hammer, K. W. Jacobsen, and J. K. Norskov, *Phys. Rev. B* **52**, 14 954 (1995).
- [27] B. Hammer and J. K. Norskov, in *Chemisorption and Reactivity on Supported Clusters and Thin Films*, edited by R. M. Lambert and G. Pacchioni (Kluwer Academic Publishers, Dordrecht, The Netherlands, 1997), p. 285 (especially Fig. 14).
- [28] J. R. Smith and T. V. Cianciolo, *Surf. Sci. Lett.* **210**, L229 (1989).